Single SPECT Measures of Cerebral Cortical Perfusion Reflect Time-Index Estimation of Dementia Severity in Alzheimer's Disease

J. Wesson Ashford, Wei-Jen Shih, John Coupal, Raj Shetty, Andrew Schneider, Cathie Cool, Ayten Aleem, Vickie H. Kiefer, Marta S. Mendiondo, and Frederick A. Schmitt

Departments of Psychiatry, Neurology, Diagnostic Radiology, and Statistics and the Alzheimer's Disease Research Center of the National Institute on Aging, Sanders-Brown Center on Aging, College of Medicine, University of Kentucky, Lexington; and Mental Health, Nuclear Medicine, Medicine, and Nursing Services, Veterans Affairs Medical Center, Lexington, Kentucky

To determine the relationship between cerebral cortical blood flow loss and the temporal development of the dementia in Alzheimer's disease (AD), SPECT was studied in a cross section of AD patients with a broad range of impairment. **Methods:** Thirty patients with a diagnosis of probable AD had their mini-mental state examination scores transformed into time-index values to give an estimation of dementia severity relative to the developmental time course. SPECT images were obtained using ^{99m}Tc-ethyl cysteinate dimer and a 3-head camera. Cortical surface perfusion was analyzed, including modified Talairach standardization, to obtain cortical elements from the convexity (each representing about 0.25 cm^2 at the surface, 6.6-mm cortical depth) referenced to the mean perfusion of the full greater cerebellar hemisphere. These element ratios were analyzed (individually and by averages of estimated Brodmann's areas and brain regions) using linear regression with the time-index value. **Results:** For individual posterotemporal and inferoparietal Brodmann's areas (21, 22 and 39, 40, respectively) the correlation coefficients between cortical perfusion ratios and dementia severity ranged between −0.67 and −0.78 ($P < 0.001$). Perfusion ratios from these regions declined 2.5%–4.2% for each estimated year of progression. Prefrontal area perfusion showed less association with severity. Perfusion in primary cortical regions had no significant association with dementia severity. **Conclusion:** Cerebral cortical perfusion loss is temporally related to development of dementia. The spatial pattern of high, significant correlations between cortical perfusion and dementia severity shows a regional distribution that corresponds closely to the distribution of AD pathology described in autopsy studies.

Key Words: Alzheimer's disease; SPECT; computer-assisted image processing; cognitive dysfunction; dementia severity

J Nucl Med 2000; 41:57–64

Alzheimer's disease (AD) is a condition that progresses over time (*1*) and impacts brain regions selectively, especially the posterotemporal and inferoparietal lobes (*2,3*). The pattern of changes in brain function can be observed with techniques that image glucose metabolism (*4–6*) or blood flow (*7–11*). These metabolic and perfusion changes correspond closely to the composite pattern of tissue degeneration seen at autopsy (*12,13*). The selective disruption of temporoparietal function seen with metabolic (*4,14,15*) or blood flow (*7–9*) imaging function is useful for confirming the AD diagnosis. Imaging techniques to identify this pattern may be useful in improving the detection of subjects early in the course of AD (*16,17*).

The general pattern of loss of temporoparietal function is not unique to AD. The same temporoparietal pattern of function loss is also seen in dementia caused by Parkinson's disease (*6,14,18–20*). However, to our knowledge, no other dementias have been found to produce this distribution.

In analyzing the relationship between regionally specific brain changes and cognition in living AD patients, investigators have reported associations between measures of dementia severity and decreases in cerebral function that are maximal in the temporal and parietal lobes, with correlations ranging from 0.4 to 0.77 (*7,21–24*). Because of the variability of the measures and the disease heterogeneity (*10*) and the imprecision of the relationship between specific neuropsychologic characteristics and local brain function deficits (*11*), controversy exists about the clinical usefulness of SPECT for the assessment of AD severity. For extending our understanding of the progression of AD and improving clinical assessment, determination of the relationship between cognitive and cerebral function in this disease is important. The explanation of this relationship depends partly on the precision and validity of the cognitive assessments and the resolution of the techniques for measuring cerebral function. One approach to improving the knowledge about this relationship is to better assess the time course of the clinical progression of the dementia in AD. Another approach is to improve the measurement techniques, using high-resolution computer image analyses with more precise quantification of cerebral cortical function.

Received Jan. 4, 1999; revision accepted May 20, 1999.

For correspondence or reprints contact: J. Wesson Ashford, MD, PhD, Department of Psychiatry, College of Medicine, University of Kentucky, 3470 Blazer Pkwy., Lexington, KY 40509.

Analysis of the association between decline of function in specific locations of the cerebral cortex and progression of dementia severity may help to improve understanding of the developmental course of AD pathology.

It has recently been suggested that dementia severity could be represented by an estimate of the mean population time course of the disease's progression (*1,25,26*). Accordingly, the nonlinear relationship between mini-mental state examination (MMSE) score and time course can be estimated by either nonparametric (*1*) or parametric (*25,26*) means. For this study, a nonparametrically fitted model was used to transform the MMSE score into time-index values as described (*1*). For example, using the MMSE score and this model of loss of cognitive function for a mean population, 0 time-index year units correspond to a MMSE score of 25, and 7 or more time-index year units of disease progression correspond to a MMSE score of 0 (*27*). This transformation has recently been used on the dataset of the Consortium to Establish a Registry for Alzheimer's Disease (*28*). In addition to modeling this nonlinear change in mental status, use of units related to time course allows an adjustment of the chronologic differences between the date of the dementia severity evaluation and the date of the SPECT scan. This study analyzes the relationship between cerebral cortical perfusion and dementia severity in patients with probable AD relative to time course and thus estimates the rate of progression of the loss of cerebral blood flow in this disease.

MATERIALS AND METHODS

Subjects

In a dementia outpatient clinic and a long-term care unit, 90 male veteran patients had a standard battery of tests, which included the MMSE (*27*) and CT and SPECT scans, over a 2-y period (May 14, 1994, to June 13, 1996). Thirty patients (mean age, 74.5 ± 5.5 y; range, 64–87 y) had a diagnosis of probable AD (National Institute of Neurological Disorders and Stroke–Alzheimer's Disease and Related Disorders Association criteria [*29*]). Patients with a history of cerebrovascular disease, or whose structural brain scans indicated stroke or other cerebrovascular or neurologic disease, did not have a diagnosis of probable AD. None of these patients had a significant history of ethanol abuse within a decade of the development of dementia. For this study of the 30 patients with probable AD, no patient was included or excluded from analysis on the basis of the SPECT pattern. For these 30 patients, there was a small, nonsignificant, positive correlation between age and MMSE score ($r = 0.19$).

MMSEs were obtained an average of +31 ± 93 d before the SPECT scans (range, −114 to +443 d; median, 13 d), and scores ranged from 0 to 25 (median, 10; 7 patients had a MMSE score = 0). These MMSE scores were transformed into time-index values using a simple nonlinear equation (*1*); an MMSE score of 25 corresponds to a time-index score of 0 (usual point of onset of clinical symptoms), and an MMSE score of 0 is defined at 7.0 y of disease progression. The time-index scores were then adjusted to the date of the SPECT scans. The mean level of severity at the time of the scans in time-index year units was 4.3 ± 2.1 (range, 0–7.3). Patients were taking various chronic medications, including psychoactive medications such as haloperidol and trazodone, which may have had some effect on cerebral blood flow. However, none of the patients was taking γ-aminobutyric acid agonists or other medications that are known to have substantial effects on cerebral function. All patients had normal levels of consciousness during MMSE and SPECT testing.

SPECT Procedures

We used a 3-head SPECT scanner (PRISM; Picker International, Inc., Cleveland Heights, OH) with high-resolution collimators. While patients lay in a quiet, dimly lit room with their eyes open, an intravenous dose (925–1110 MBq) of ^{99m}Tc-ethyl cysteinate dimer (ECD) (≥90% radiochemical purity, Neurolite; DuPont Merck Pharmaceuticals, Billerica, MA) was administered. ^{99m}Tc-ECD has uptake characteristics that make it a satisfactory marker for measuring regional cerebral blood flow in AD and is best for maximizing image contrast and quality (*30*). ECD provides a high signal and is rapidly cleared from extracerebral tissue, yielding images suitable for computer analysis (*31*). This agent produces tracer concentrations in AD brains that are proportional to blood flow (*32*). Furthermore, it is suitable for diagnostic assessment, providing information that is useful for determining the degree of functional brain impairment in AD patients (*33*).

Thirty minutes after ECD injection, SPECT images were obtained (2.2 × 2.2 mm resolution, 128 pixels wide, 120 images, 30 s/image, continuous camera motion during data collection) with no corrections for attenuation. Raw data images were backprojected onto 128 × 128 horizontal matrices (ramp prefilter followed by a low-pass filter with order of 4.0 and cutoff frequency of 0.3; voxel size, 2.2 × 2.2 × 2.2 mm; resolution, 6.7 mm at 15-cm full width at half maximum).

Between-patient SPECT comparisons usually use the cerebellum as a reference (*15,34*). In AD, loss of blood flow probably occurs in the cerebellum, leading to an underestimation of the magnitude of the disease effect in structures being referenced (*32*). In this study the values of cortical surface elements were divided by the average perfusion of the full volume of the cerebellar hemisphere with the greater average value to obtain cortical perfusion ratios (CPRs).

Cortical surface analysis used parallel rays directed at the horizontal matrices to find the cortical surface (Figs. 1A and 1B). The cortical surface was defined as the first set of 3 consecutive points on the ray whose average exceeded a threshold of 35% of the value of the greater cerebellar hemisphere (although the starting point of the ray and the threshold could be adjusted to improve image quality). This average value was taken to represent the local cortical perfusion value. This method is similar to that described by Tachibana et al. (*18*), except parallel rays were used in the current study to find the surface, whereas the study by Tachibana et al. (*18*) used elliptic rays (we are currently developing a method that uses ovoid rays). For image viewing, 8 sets of parallel rays were directed at the brain, 1 set from each side (Figs. 1A, 1C, and 1E), superior and posterior, anterior and posterior, and outward laterally from an estimated medial plane (Figs. 1A, 1B, 1D, and 1F). Curved edge limits were compared between adjacent dimensions to reduce tangent artifacts (Fig. 1B), and threshold adjustments were used to improve resolution. The resulting views were assembled as a perfusion picture (Figs. 1C and 1D for left lateral and right medial views, respectively) and a surface 3-dimensionally rendered picture (Figs. 1E and 1F for left lateral and right medial views, respectively). The lateral surface structural images allowed visualization of external anatomic landmarks of the brain, such as the

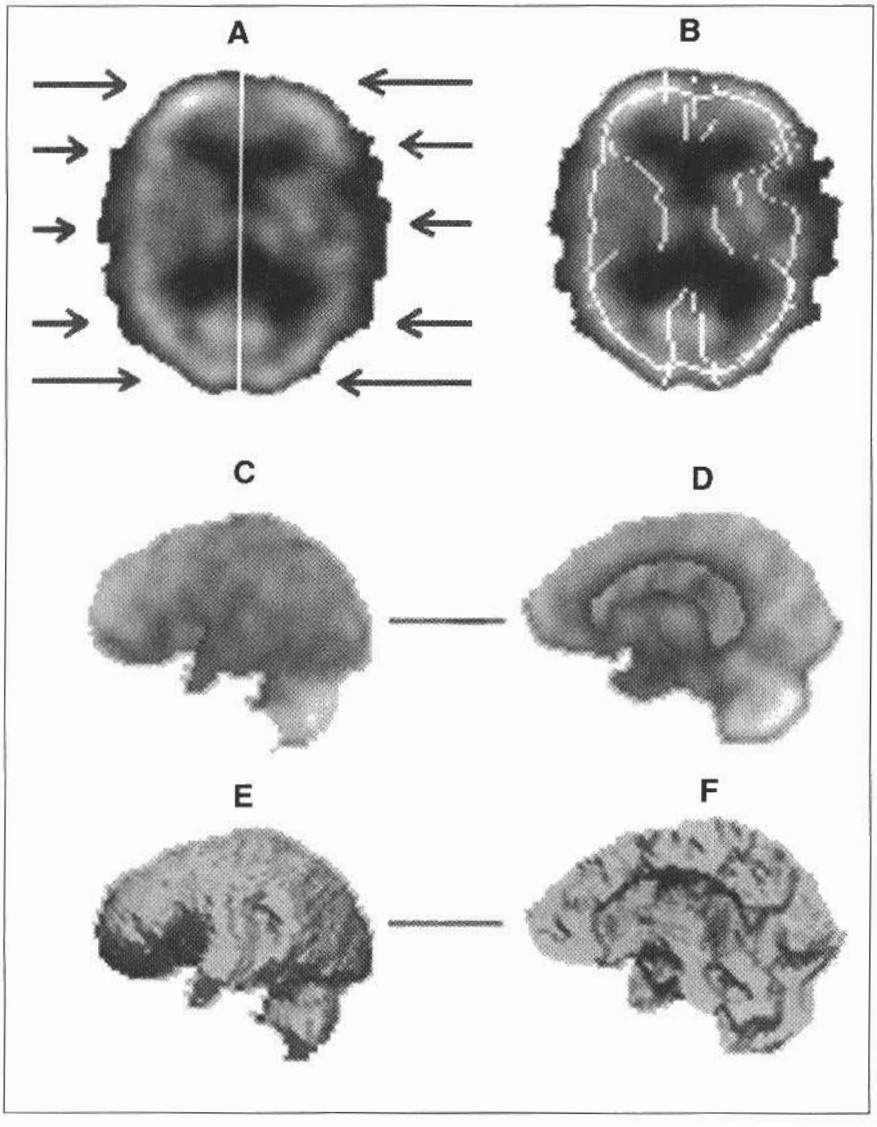

FIGURE 1. Cortical surface determination. (A and B) Horizontal matrices are analyzed by parallel rays (A, lateral rays are directed medially) to estimate cortical surface (B, lateral and medial surface estimates for both left and right hemispheres). (C and D) Raw, surface, cerebral perfusion values from across all horizontal matrices are used to construct cerebral perfusion pictures. (E and F) Information about location of surface values is used to construct 3-dimensional surface picture.

sylvian sulcus. The medial views portrayed the brain stem, the void of the corpus callosum just below the cingulate gyrus, the approximate location of the posterior commissure, and the suggested location of the anterior commissure (Figs. 1D and F).

Morphologic standardization was a modification of the Talairach and Tournoux procedure (*35*), applied to only the lateral views, left and right (Fig. 2). The line connecting the anterior and posterior commissure coordinates was estimated using the medial image processed by the 3-dimensional rendering algorithm. Because of the lack of clarity of the anterior commissure, reference was made to the external orientation of this line in Talairach and Tournoux's atlas (*35*) and the lateral images of the 3-dimensionally rendered external surface images to verify the position of this line. Because the anterior commissure frequently lies anterior to the tip of the atrophic temporal lobe of the AD brain (a violation of Talairach and Tournoux's morphometry), the tip of the temporal lobe was used as the midanterior limit instead of the anterior commissure, with separate adjustments for the left and right hemispheres. The cerebellum was then removed by estimating the boundary between the inferior aspect of the cerebrum on the lateral view (Fig. 2A). The full volume of each cerebellum between the lateral points and the estimated midline (Fig. 1A) was analyzed to define the mean voxel count values for each cerebellar hemisphere. The greater of the 2 values was used as the denominator for calculating the surface ratios of the cortical surface elements. Then the brain was stretched, using the established landmarks, to meet the standard outline (Fig. 3). Voxels from the raw image ($2.2 \times 2.2 \times 2.2$ mm) were grouped to form a standard size, resulting in the derived elements (each representing about 0.25 cm^2 at the surface, 6.6-mm cortical depth), presented in CPRs (Fig. 2B).

Statistical Analysis

The derived elements from the 2 hemispheres were transformed into a columnar matrix containing 1330 CPRs for each patient (representing a surface area of about 333 cm^2). On the basis of the description in Talairach and Tournoux's atlas (*35*), these CPRs were averaged for each Brodmann's area (Fig. 3) and for larger lobar regions (prefrontal, posterotemporal and inferoparietal, primary somatic) bilaterally (Table 1). We performed least-squares linear regressions of the average CPR for each CPR element, for 26 Brodmann's areas bilaterally (for each patient), and for these 3 global regions as a function of the time-index values (derived from

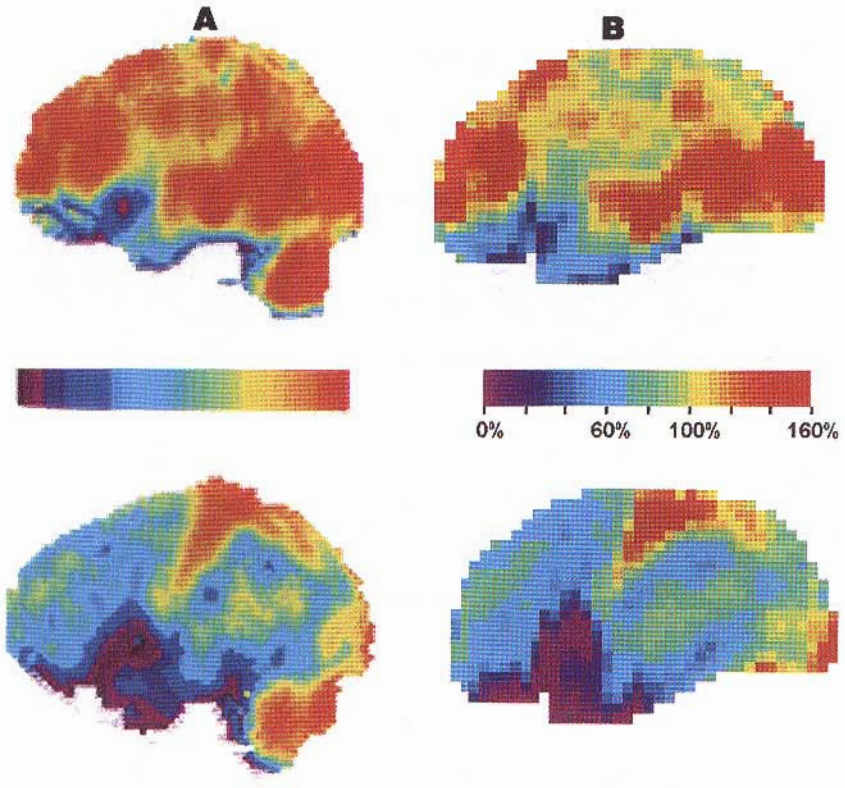

FIGURE 2. Cerebral perfusion image standardization. (A) Raw cerebral perfusion images are shown (highest value represents maximum value in dataset, far right on scale; pixels are 2.2 × 2.2 mm). (B) Values are transposed into lateral Talairach and Tournoux representation (*35*) (scale represents cerebral perfusion ratios relative to full greater cerebellar average raw-perfusion value).

the MMSE scores). The values from these calculations were used to assess the rate of decline in cerebral blood flow associated with increasing dementia severity. Correlations were examined to estimate the spatial distribution of CPR loss, to compare the degree of correlation between specific areas and regions, and to determine the significance of this loss.

RESULTS

A visual representation of the individual correlation coefficients for each surface element is shown superimposed on the Brodmann's areas from Talairach and Tournoux's atlas (*35*) (Fig. 4) to show the general distribution of the relationships between the CPRs and the time-index severity measures. The general pattern of correlations between cerebral blood flow and dementia severity (Fig. 4) suggested a negative relationship between CPRs and dementia severity that was most pronounced in the temporal and parietal regions, intermediate in the prefrontal regions, and minimal or positive in the primary regions. For most cortical elements in the temporal and parietal regions, regression values ranged from −0.40 to −0.80 (Fig. 4).

The posterotemporal or inferoparietal regions bilaterally showed a correlation between blood flow and dementia severity of −0.79 (Fig. 5A), with correlation coefficients for the individual Brodmann's areas in these regions ranging from −0.66 to −0.78 ($P < 0.01$) (Table 2). As expected, these results indicate that AD has a major impact on the posterotemporal and inferoparietal regions. Furthermore, the pattern of correlations (Fig. 4) indicates that the impact is distributed broadly across this relatively homogeneous associative cortex.

A correspondence was found between the rates of decline of the CPRs (calculated by least-squares regression) and the

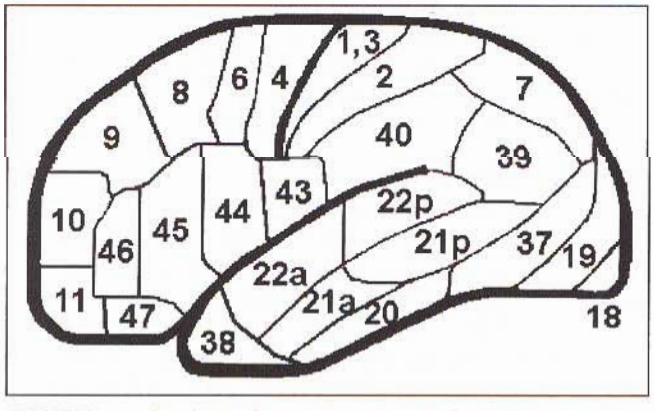

FIGURE 3. Brodmann's areas, adapted from Talairach and Tournoux (*35*). Areas 21 and 22 are divided into anterior (a) and posterior (p) sections.

TABLE 1
Brodmann's Areas of Designated Lobar Regions

Region	Brodmann's areas
Posterotemporal and inferoparietal	21p, 22p, 39, 40
Prefrontal	8–11, 46
Primary somatic (around central sulcus)	1, 3, 4

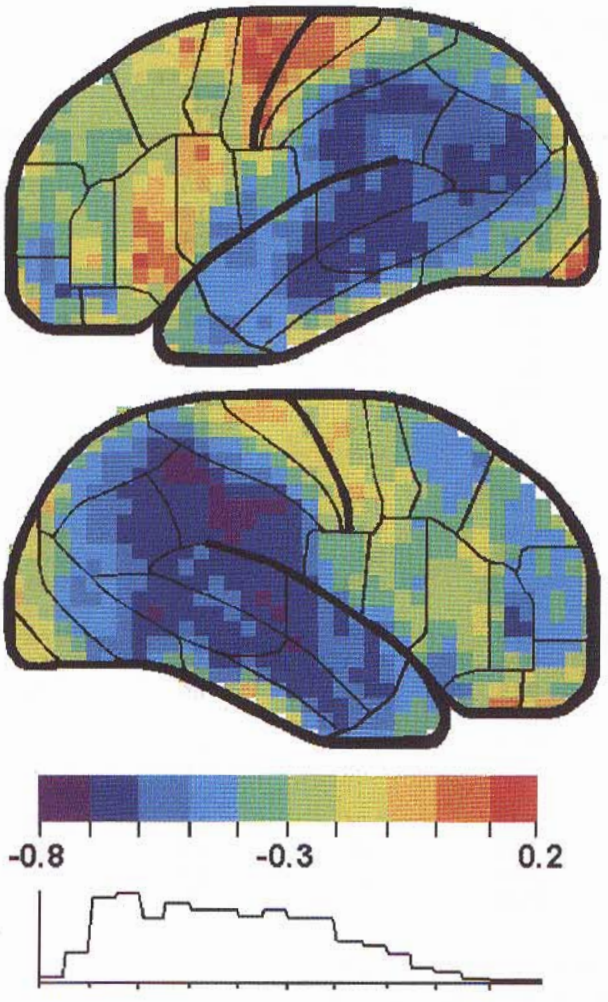

FIGURE 4. Lateral view of cortical surface (left side is on top). Scale indicates range for Pearson correlations with single decimal precision. Bottom graph shows relative frequency of each decimal range.

associated correlation coefficients between dementia severity and CPRs across all Brodmann's areas, with more rapid rates occurring in the areas with the higher correlations (Table 2). For example, the Brodmann's areas of the posterotemporal and inferoparietal regions showed rates of decline of 2.5%–4.3%/y (Table 2) and a rate of 3.3%/y for this region as a whole. Consequently, the CPR for this region decreased by 27% (from 1.08 to 0.80) for the time-indexed 7 y (MMSE decline from 25 to 0) between mild and severely impaired patients (Fig. 5A).

Generally, intermediate associations were found between severity and CPRs in the prefrontal areas (Fig. 5B; Table 2). The correlation with the average CPR for this region bilaterally was −0.53, and the least-squares linear regression showed a decline rate of 1.7%/y (Fig. 5B). Consistent with an observation reported earlier (*21*), there seemed to be more variability in the CPRs of the more severely impaired patients in these areas (note the increased dispersion of the values for the more impaired patients in Fig. 5B).

The CPRs in the primary somatic cortical regions (Fig. 5C) and the lateral visual areas of the occipital cortex (area 18) showed low correlations with severity, suggesting less change in CPR with the advance of AD. Another region relatively unaffected was Broca's speech area (Brodmann's areas 44 and 45 on the left side of the brain). The primary visual cortex, at the tip of the occipital lobe and medially

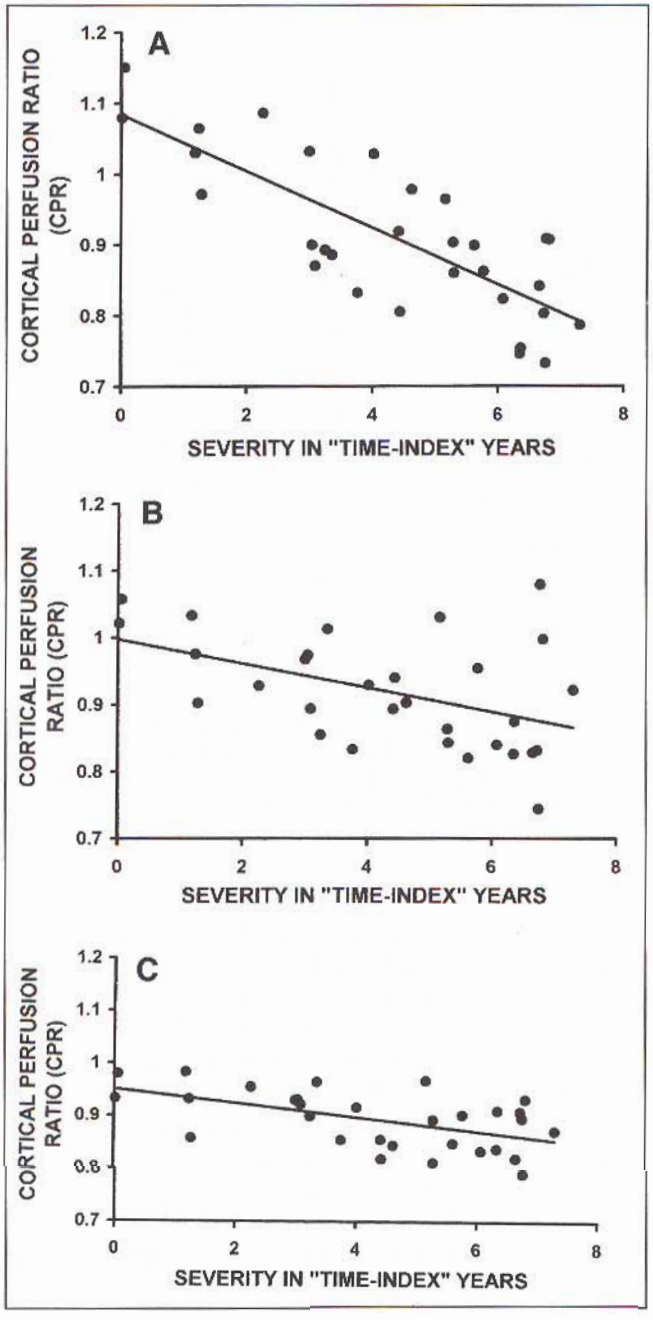

FIGURE 5. CPR values for regions (bilateral), plotted by time-index values for each patient; solid line is least-squares regression. (A) Posterotemporal (areas 21 and 22) and inferoparietal (areas 39 and 40); intercept = 1.08; slope = −3.3%/y; $r = -0.79$ ($P < 0.0001$). (B) Prefrontal (areas 8–11 and 46); intercept = 1.0; slope = −1.7%/y; $r = -0.53$ ($P < 0.01$). (C) Central gyri (areas around central sulcus) (areas 1, 3, and 4); intercept = 0.95; slope = −0.4%/y; $r = -0.14$ ($P > 0.05$).

TABLE 2
Correlation Between Dementia Severity and CPRs for Brodmann's Areas

Brodmann's area	n	Left hemisphere			Right hemisphere		
		Intercept	Slope	r^*	Intercept	Slope	r^*
Parietal							
39	36	0.91	−3.1	−0.69	0.95	3.6	−0.66
40	48	0.87	−2.9	−0.68	0.94	−3.9	0.78
7	28	0.86	1.9	−0.51	0.91	−2.4	−0.54
Temporal							
21p	30	0.91	−3.8	−0.71	0.95	−4.3	−0.71
22p	30	0.90	−3.3	−0.70	0.96	−4.3	0.72
21a	21	0.80	−2.8	−0.67	0.87	−3.8	0.72
22a	37	0.83	−2.5	−0.67	0.87	−3.5	−0.75
37	33	0.88	−2.2	0.56	0.92	−2.8	−0.59
20	20	0.68	−1.4	−0.55	0.73	−1.8	−0.56
38	21	0.64	−1.5	−0.50	0.66	−2.3	−0.56
Frontal							
11	30	0.77	−1.8	−0.57	0.78	−1.5	−0.40
10	26	0.93	−1.8	−0.44	1.00	−2.6	−0.50
47	13	0.59	−1.1	−0.43	0.59	−1.1	−0.41
46	19	0.81	1.3	−0.41	0.88	−2.2	−0.56
9	33	0.85	−1.4	−0.38	0.79	−1.6	−0.43
44	31	0.75	−1.0	−0.28	0.78	−1.6	−0.43
8	32	0.80	−0.9	−0.24	0.83	2.1	−0.54
45	38	0.68	0.5	−0.18	0.72	−1.4	0.44
Occipital							
19	25	0.88	−1.4	−0.31	0.91	−1.5	−0.35
18	5	0.85	0.4	0.08	0.93	−1.0	−0.20
Central							
43	18	0.84	1.7	−0.49	0.84	−2.0	−0.53
2	35	0.85	−1.4	−0.42	0.88	−2.1	0.49
6	19	0.83	−0.9	−0.25	0.83	−1.2	−0.33
1, 3, 4	47	0.84	0.0	−0.01	0.86	−0.7	−0.23

*For n = 30, 1-tailed tests indicate $r = -0.36$, $P = 0.05$; $r = -0.46$, P 0.01; $r = -0.57$, $P = 0.001$.
n = number of cortical SPECT elements in each Brodmann's area; r = Pearson correlation coefficient.
Linear regression results are given for CPRs of Brodmann's areas (arranged by cerebral region) versus time-index values. Intercept is calculated CPR (cortical blood flow ratio) at time index = 0 from least-squares linear regression line with slope calculated in units of %/y (loss in flow relative to that of cerebellum).

along the banks of the calcarine fissure, was similarly unaffected (Fig. 4, medial data not shown). Those patients with the most severe dementia still showed relatively normal blood flow ratios in all primary regions. The values of the correlation coefficients increased progressively from the primary regions through the corresponding secondary regions to the associative cortical areas (Fig. 4).

The calculated CPRs for all of these areas at the defined threshold of clinically observable dementia (time index = 0) showed small differences. None of the discrepancies between the intercepts was considered to significantly influence the correlation and rate analyses.

DISCUSSION

The aim of this study was to determine the relationship between cortical blood flow and the time-course of AD progression using cross-sectional data. Consistent with previous findings, impairment of CPRs was associated with dementia severity (*7,15,23,24*). Furthermore, these data showed highly significant correlations between blood flow losses in specific Brodmann's areas and the time course of dementia development. As expected, the most rapid decline of perfusion developed in the posterotemporal and inferoparietal areas of these patients. Flow changes in the frontal regions appear to develop at intermediate and variable rates, and no significant hypoperfusion develops in the primary cortical regions.

A notable geographic variation occurred between the pattern of Brodmann's areas affected in the right prefrontal regions (areas 8, 10, and 46) and the 1 prefrontal area on the left side (area 11). This pattern suggests that future studies of neuropathologic and functional brain changes in AD patients should report both left and right hemisphere results.

Several studies have used correlation analyses or linear regression to examine functional imaging measures and their association with clinical symptoms as measured by different dementia rating scales (*8,10,11,17,36*). In early cases of AD,

these scales have complex interactions with dementia severity (e.g., ceiling effects and education effects). Thus, a better method of dementia severity assessment is needed to grade progression of AD, especially for mildly demented patients. Brain scan analyses could help in the development of early assessment measures.

The mean time course of AD provides a framework to develop a transformation of any measure of dementia signs or symptoms, which are progressive in a defined population with AD, into a standard interval scale. Using values on a time-index scale, changes in mild ranges can be compared with changes in severe ranges using identical interval units (of time). In these analyses, rates of progression of blood flow loss over time could be estimated from cross-sectional data. The correlations between CPRs and dementia severity in posterotemporal and inferoparietal regions were as high as −0.79, meaning that the least-squares regression line explains 63% of the change in CPRs. These correlations are comparable with those found between different psychometric tests used to assess dementia severity (*36*).

A further issue is explanation of the variance in CPR data unexplained by dementia severity. Because of the concern that age could have contributed to this relationship, the correlation between age and MMSE score was examined. Age had a nonsignificant (slightly positive) correlation with MMSE score in this sample. Therefore, an age effect is unlikely to have affected the relationship between dementia severity and CPR. Also, because the relationship between age and MMSE score was (slightly) positive (older age, better score), the known relationship between age increase and CPR decline could not contribute to these findings. Similarly, cerebellar blood flow is believed to decline slightly over the course of AD, so use of the cerebellum as the reference would be expected to weaken, not contribute to, the findings (*32*). Because this study examined the cortical surface, correction for lobar atrophy was not required. AD is accompanied by minimal cortical thinning that could explain only a small part of the results. No other cerebral blood flow measurement factor, such as attenuation, was considered as a possible cause of the described correlation, but some such factor could have influenced the results.

In considering other possible explanations of the relationship between CPRs and illness time course, some unexplained variance could be associated with a wide range of patient factors. Prescribed centrally or peripherally active medications could have affected the SPECT values, including the variations in frontal lobe function, but few patients were taking medications, and those medications that were prescribed are not known to have such dramatic effects. Other factors include variability in performance on the MMSE; variations in brain anatomy and Brodmann's area location; disease-related issues, including genetics and environmental stresses; variation in the exact pattern of areas affected by the AD process; or concurrent additional neurodegenerative disease processes. Additional factors that could have affected the correlation include premorbid brain size or psychosocial variables, including education (*37*). More precise testing (*21,22,38*) and multidimensional testing (*8–11,36*) may also account for additional currently unexplained variations in the relationship between cerebral blood flow and dementia severity.

Prior studies suggest a pattern of sequential attack by AD of temporoparietal before frontocortical regions based on neuropathologic analysis (*2*) and metabolic brain scan results (*21,39*). These data indicate that the disease process does affect particular regions more severely according to the hierarchy of involvement suggested by the distribution of neurofibrillary pathology (*2*). However, more precise longitudinal studies are needed to define whether the attack is temporally sequential or related to a hierarchy of vulnerability (*1,38*). In the involved brain regions, AD pathology destroys neuronal processes (*40*). Presumably, the loss of metabolic demand associated with the loss of these processes causes the decrease in cerebral blood flow. Alternatively, other mechanisms, such as loss of projecting connections from activating regions, may account for such a decrease in intact structures, which could later contribute to the development of pathology in these structures.

This study shows that analysis of cerebral blood flow in patients with AD can help to determine the progression of AD and thereby may be useful for further understanding the evolution of the disease process, developing more reliable diagnosis, and testing new therapies. Multicenter SPECT studies of AD patients, particularly with respect to the time course of the disease, would help to clarify the usefulness of this tool, and the area in most need of study is the early phases preceding the dementia.

CONCLUSION

This study shows that SPECT data reflect the progressive loss of cerebral cortical blood flow in various brain regions relative to the time course of AD. Because the time-index method could be applied to any psychometric test used to assess dementia severity, it provides a framework to analyze disease progression across the full spectrum of AD and to make comparisons across different studies. Such analyses could be used as a standard to evaluate psychologic or radiologic tools that are needed to measure dementia severity and progression, especially for the investigation of treatment interventions and potential etiologic factors.

A similar correlation occurs between a clinical quantitation of 3-dimensional SPECT scans and interscan intervals to follow-up scans (*41*).

ACKNOWLEDGMENTS

This research was supported in part by National Institutes of Health grants AG 05144 and AG 10483 and the Department of Veterans Affairs. ECD was generously provided by DuPont Pharma Radiopharmaceuticals (North Billerica, MA).

REFERENCES

1. Ashford JW, Shan M, Butler S, Rajasekar A, Schmitt FA. Temporal quantification of Alzheimer's disease severity: 'time-index' model. *Dementia*. 1995;6:269–280.
2. Braak H, Braak E. Neuropathological staging of Alzheimer-related changes. *Acta Neuropathol*. 1991;82:239–259.
3. Geddes JW, Tekirian TL, Soultanian NS, Ashford JW, Davis DG, Markesbery WR. Comparison of neuropathologic criteria for the diagnosis of Alzheimer's disease. *Neurobiol Aging*. 1997;18:S1–S7.
4. Burdette JH, Minoshima S, Vander Borght T, Tran DD, Kuhl DE. Alzheimer disease: improved visual interpretation of PET images by using three-dimensional stereotaxic surface projections. *Radiology*. 1996;198:837–843.
5. Minoshima S, Frey KA, Koeppe RA, Foster NL, Kuhl DE. A diagnostic approach in Alzheimer's disease using three-dimensional stereotactic surface projections of fluorine-18-FDG PET. *J Nucl Med*. 1995;36:1238–1248.
6. Kuhl DE, Metter EJ, Benson DF, et al. Similarities of cerebral glucose metabolism in Alzheimer's and Parkinsonian dementia. *J Cereb Blood Flow Metab*. 1985;5: S169–S170.
7. Jobst KA, Hindley NJ, King E, Smith AD. The diagnosis of Alzheimer's disease: a question of image? *J Clin Psychol*. 1994;55(suppl 11):22–31.
8. Hirsch C, Bartenstein P, Minoshima S, et al. Reduction of regional cerebral blood flow and cognitive impairment in patients with Alzheimer's disease: evaluation of an observer-independent analytic approach. *Dementia Geriatr Cogn Dis*. 1997;8: 98–104.
9. Bartenstein P, Minoshima S, Hirsch C, et al. Quantitative assessment of cerebral blood flow in patients with Alzheimer's disease by SPECT. *J Nucl Med*. 1997;38:1095–1101.
10. Green JDW, Miles K, Hodges JR. Neuropsychology of memory and SPECT in the diagnosis and staging of dementia of Alzheimer type. *J Neurol*. 1996;243:175–190.
11. Sabbagh MN, Lynn P, Jhingran S, et al. Correlations between SPECT regional cerebral blood flow and psychometric testing in patients with Alzheimer's disease. *J Neuropsychiatry Clin Neurosci*. 1997;9:68–74.
12. Friedland RP, Brun A, Budinger TF. Pathological and positron emission tomographic correlations in Alzheimer's disease. *Lancet*. 1985;1:228.
13. DeCarli C, Atack JR, Ball MJ, et al. Post-mortem regional neurofibrillary tangle densities but not senile plaque densities are related to regional cerebral metabolic rates for glucose during life in Alzheimer's disease patients. *Neurodegeneration*. 1992;1:113–121.
14. Gilman S. Imaging the brain. *N Engl J Med*. 1998;338:889–894.
15. Herholz K. FDG PET and differential diagnosis of dementia. *Alzheimer Dis Assoc Disord*. 1995;9:6–16.
16. Bottino CMC, Almeida OP. Can neuroimaging techniques identify individuals at risk of developing Alzheimer's disease? *Int Psychogeriatr*. 1997;9:389–403.
17. Johnson KA, Jones K, Holman BL, et al. Preclinical prediction of Alzheimer's disease using SPECT. *Neurology*. 1998;50:1563–1571.
18. Tachibana H, Kawabata K, Tomino Y, Sugita M, Fukuchi M. Brain perfusion imaging in Parkinson's disease and Alzheimer's disease demonstrated by three-dimensional surface display with ^{123}I-iodoamphetamine. *Dementia*. 1993;4:334–341.
19. Read SL, Miller BL, Mena I, Kim R, Itabashi H, Darby A. SPECT in dementia: clinical and pathological correlation. *J Am Geriatr Soc*. 1995;43:1243–1247.
20. Vander Borght T, Minoshima S, Giordani B, et al. Cerebral metabolic differences in Parkinson's and Alzheimer's diseases matched for dementia severity. *J Nucl Med*. 1997;38:797–802.
21. Haxby JV, Grady CL, Koss E, et al. Heterogeneous anterior-posterior metabolic patterns in dementia of the Alzheimer type. *Neurology*. 1988;38:1853–1863.
22. Schmitt FA, Shih W-J, DeKosky ST. Neuropsychological correlates of single photon emission computed tomography (SPECT) in Alzheimer's disease. *Neuropsychology*. 1992;6:159–171.
23. Smith GS, de Leon MJ, George AE, et al. Topography of cross-sectional and longitudinal glucose metabolic deficits in Alzheimer's disease. *Arch Neurol*. 1992;49:1142–1150.
24. Mielke R, Herholz K, Grond M, Kessler J, Heiss WD. Clinical deterioration in probable Alzheimer's disease correlates with progressive metabolic impairment of association areas. *Dementia*. 1994;5:36–41.
25. Liu X, Tsai W-Y, Stern Y. A functional decline model for prevalent cohort data. *Stat Med*. 1996;15:1023–1032.
26. Stern Y, Liu X, Albert M, et al. Application of a growth curve approach to modeling the progression of Alzheimer's disease. *J Gerontol*. 1996;51:M179–M184.
27. Folstein MF, Folstein SE, McHugh PR. "Mini-Mental State": a practical method for grading the cognitive state of patients for the clinician. *J Psychol Res*. 1975;12:189–198.
28. Mendiondo MS, Ashford JW, Kryscio RJ, Schmitt FA. Modeling Mini-Mental State Exam changes in Alzheimer's disease. *Stat Med*. 2000: in press.
29. McKhann C, Drachman D, Folstein M, Katzman R, Price D, Stadlan EM. Clinical diagnosis of Alzheimer's disease: report of the NINCDS-ADRDA Work Group under the auspices of Department of Health and Human Services Task Force on Alzheimer's Disease. *Neurology*. 1984;34:939–944.
30. Slosman DO, Magistretti PJ. Cerebral SPECT imaging: advances in radiopharmaceuticals and quantitative analysis. In Becker R, Giacobini E, eds. *Alzheimer Disease: From Molecular Biology to Therapy*. Boston, MA: Birkhauser; 1996:445–450.
31. Johnson B, Lamki L, Fang B, et al. Demonstration of dose-dependent global and regional cocaine-induced reductions in brain blood flow using a novel approach to quantitative single photon emission computerized tomography. *Neuropsychopharmacology*. 1998;18:377–384.
32. Darcourt J, Migneco O, Robert P, Benoit M. SPECT scan and efficacy of therapy in Alzheimer's disease. In Becker R, Giacobini E, eds. *Alzheimer Disease: From Molecular Biology to Therapy*. Boston, MA: Birkhauser; 1996:457–461.
33. Waldemar G, Walovitch RC, Andersen AR, et al. ^{99m}Tc-bicisate (Neurolite) SPECT brain imaging and cognitive impairment in dementia of the Alzheimer type: a blinded read of image sets from a multicenter SPECT study. *J Cereb Blood Flow Metab*. 1994;14(suppl. 1):S99–S105.
34. Minoshima S, Frey KA, Foster NL, Kuhl DE. Preserved pontine glucose metabolism in Alzheimer disease: a reference region for functional brain image (PET) analysis. *J Comput Assist Tomogr*. 1995;19:541–547.
35. Talairach J, Tournoux P. *Co-Planar Stereotaxic Atlas of the Human Brain*. New York, NY: Thieme Medical Publishers; 1988.
36. Ashford JW, Kumar V, Barringer M, et al. Assessing Alzheimer severity with a global clinical scale. *Int Psychogeriatr*. 1992;4:55–74.
37. Butler SM, Ashford JW, Snowdon DA. Age, education, and changes in the Mini-Mental State Exam scores of older women: findings from the Nun study. *J Am Geriatr Soc*. 1996;44:675–681.
38. Eberling JL, Reed BR, Baker MG, Jagust WJ. Cognitive correlates of regional cerebral blood flow in Alzheimer's disease. *Arch Neurol*. 1993;50:761–766.
39. Eberling JL, Jagust WJ, Reed BR, Baker MG. Reduced temporal lobe blood flow in Alzheimer's disease. *Neurobiol Aging*. 1992;13:483–491.
40. Ashford JW, Soulatanian NS, Zhang S-X, Geddes JW. Neuropil threads are collinear with MAP2 immunostaining in neuronal dendrites of Alzheimer brain. *J Neuropathol Exp Neurol*. 1998;57:972–978.
41. Shih W-J, Ashford JW, Coupal JJ, et al. Consecutive brain SPECT surface three-dimensional displays show progression of cerebral cortical abnormalities in Alzheimer's disease. *Clin Nucl Med*. 1999;24:773–777.